Available online at BCREC Website: http://bcrec.undip.ac.id

Bulletin of Chemical Reaction Engineering & Catalysis, 9 (3), 2014, 192-200

Research Article

Isothermal Kinetics of Diesel Soot Oxidation over $La_{0.7}K_{0.3}ZnO_y$ Catalysts

R. Prasad, Abhishek Kumar, Anupama Mishra*

Department of Chemical Engineering and Technology, IIT (BHU), Varanasi-221005, Uttar Pradesh, India

Received: 26th April 2014; Revised: 27th May 2014; Accepted: 28th June 2014

Abstract

This paper describes the kinetics of catalytic oxidation of diesel soot with air under isothermal conditions (320-350 °C). Isothermal kinetics data were collected in a mini-semi-batch reactor. Experiments were performed over the best selected catalyst composition $La_{0.7}K_{0.3}ZnO_y$ prepared by sol-gel method. Characterization of the catalyst by XRD and FTIR confirmed that $La_{1-x}K_xZnO_y$ did not exhibit perovskite phase but formed mixed metal oxides. 110 mg of the catalyst-soot mixture in tight contact (10:1 ratio) was taken in order to determine the kinetic model, activation energy and Arrhenius constant of the oxidation reaction under the high air flow rate assuming pseudo first order reaction. The activation energy and Arrhenius constant were found to be 138 kJ/mol and 6.46×10^{10} min^{-1}, respectively.

Keywords: Soot emissions; mixed metal oxide; Soot oxidation; Isothermal kinetics

How to Cite: Prasad, R., Kumar, A., Mishra, A. (2014). Isothermal Kinetics of Diesel Soot Oxidation over $La_{0.7}K_{0.3}ZnO_y$ Catalysts. *Bulletin of Chemical Reaction Engineering & Catalysis*, 9(3): 192-200. (doi: 10.9767/bcrec.9.3.6773.192-200)

Permalink/DOI: http://dx.doi.org/10.9767/bcrec.9.3.6773.192-200

1. Introduction

During the last decade, diesel engines have increased in popularity compared to gasoline engines all around the world, due to better fuel efficiency, lower operating cost, higher durability, and reliability, simultaneously associated with a favourable fuel tax situation in several countries. They are energy efficient, durable, and drivable but their emissions of particulate matter (PM) or soot and NO_x are responsible of severe environmental and health problems [1]. Specifically, diesel PM has led the legislation to adopt stringent emission standards. Diesel particulate filters (DPF) are becoming widespread as an effective measure to reduce soot emissions from diesel vehicles as they have filtration efficiencies of almost 100%. As the filters accumulate PM, it builds up back pressure that has many negative effects such as decreased fuel economy and possible engine and/or filter failure [2]. To prevent these negative effects, the DPF has to be regenerated periodically, i.e. the combustion of the accumulated soot.

It is therefore, vital to understand the regeneration process in order to optimize the application and operation of DPF both for lifetime durability and fuel economy purposes. However, diesel soot elimination is known to be a hard task, since this material burns at around 600 °C with air, while diesel exhaust gases temperature most of the time lies between 150-450 °C. Therefore, some artifice is needed to promote soot oxidation. Very often this is carried out by the use of an oxidation catalyst

* Corresponding Author
E-mail: amishra.rs.che12@itbhu.ac.in (A. Mishra)
Telp: +918171257955

based DPF [3] in order to lower the required combustion temperatures.

The performance of catalytic traps is affected by the intrinsic catalytic activity and the soot-catalyst contact efficiency [4]. The nature of the contact between soot and the catalyst depends on two important parameters: the relative concentration of the solids and the mixing method. In experimental studies the soot-catalyst mixture, in an appropriate ratio, are milled in an agate mortar for "tight contact" or mixed carefully with a spatula for "loose contact" [5]. In most of the studies reported in the literature, the catalyst performances are based on the light-off temperatures. The comparison of the catalyst performances may be consistent within one set of data, but the differences in the experimental conditions such as the heating rates and the gas flow rates may cause differences in the light-off temperatures. A better tool for catalyst performance comparison is to report the activation energy for the process [6]. Furthermore, the activation energy data are needed for the modelling and design of the catalytic soot converters.

Despite the significant progress in soot oxidation studies and the extended literature, there is still high uncertainty concerning the corresponding kinetic equations. Great scatter is observed regarding the reported activation energy (E), the order of reaction with respect to both the oxidants and the running soot mass [7, 8] in the oxidation reaction. The reported activation energy (E) of the various soot-catalyst

Table 1. Reported activation energy for catalytic soot oxidation at a glance

Ref	Cat. preparation method	Experimental	Operating parameter	E (kJ/mol)
[8]	0.4% Pt/Ce-ZrO_2 impregnation	TPO, 700 mg soot/catal = 1:20, loose contact	Heated 5 ^oC/min, air flow 300 ml/min, isothermal	161
[32]	1% Pt/Al_2O_3 impregnation	TPO, 500 mg soot/catal = 1:9, loose contact	Heated 2 ^oC/min, air flow 50 ml/min, non- isothermal	161
[32]	1% Pt/CeO_2 impregnation	TPO, 500 mg soot/catal = 1:9, loose contact	Heated 2 ^oC/min in air flow 50 ml/min, non- isothermal	154
[32]	1% Pt/La_2O_3 impregnation	TPO, 500 mg soot/catal = 1:9, loose contact	Heated 2 ^oC/min in air flow 50 ml/min, non- isothermal	147
[32]	1% Pt/SiO_2 impregnation	TPO, 500 mg soot/catal = 1:9, loose contact	Heated 2 ^oC/min in air flow 50 ml/min, non- isothermal	159
[32]	1% Pt/ZrO_2 impregnation	TPO, 500 mg soot/catal = 1:9, loose contact	Heated 2 ^oC/min in air flow 50 ml/min, non- isothermal	158
[33]	Mn_2O_3	TGA, Soot/Mn = 9:1 Soot doped with Mn-acetate	Heated 1.5-7.5 oC/min in air flow 50 ml/min, non-isothermal	107
[34]	$LaCrO_3$, $La_{0.9}CrO_3$, $La_{0.8}CrO_3$, $La_{0.9}Rb_{0.1}CrO_3$, $La_{0.9}Na_{0.1}CrO_3$, $La_{0.9}K_{0.1}CrO_3$, $La_{0.8}Cr_{0.9}Li_{0.1}O_3$ Soln. combustn.	TGA, Soot/catal = 1/2 tight contact	Different heating rates (Φ = 5, 10, 20, 30, and 40 ^oC/min) air flow of 100 ml/min,	142 128 123 119 129 114 115
Present Study	$La_{0.7}K_{0.3}ZnO_y$	Semi batch, 110 mg soot/catal = 1/10 tight contact	Isothermal, 320-350 ^oC, air flow 150 ml/min	138

mixtures is given in Table 1. The basic reasons, which lead to those discrepancies, are related with the soot samples, type of catalysts, soot catalyst contacts and experimental setup characteristics. The commonly used synthetic soot samples are not necessarily equivalent to real diesel soot. Then again the quality of real soot is not constant and depends on engine and operational parameters. And finally, the experimental setup itself may impose uncertainties, such as rate controlling mass transfer limitations, etc.

Different experimental approaches have been used in the literature including thermogravimetric analysis (TG) [9, 10], flow reactor [11], semi-batch fixed bed reactor [8]. Several studies [12-14] on the kinetics of non-catalytic and catalytic soot oxidation have been reported in the literature. It is concluded that more detailed insight in the kinetics and mechanism of soot oxidation might help in developing more active and selective soot oxidation catalysts and in modelling of catalytic DPF [8, 15].

A platinum group metals (PGM) coated DPF has been presented as an efficient after-treatment system [16]. But in recent years, considering the high cost, limited availability of the noble metals and their instability with impurities, more attention has been focused on the metal oxide perovskite structure [17-19] and mixed metal oxide [20, 21] catalysts. Vast literature is available for the oxidation of soot over various catalysts. The addition of alkali metal acts as a catalyst promoter and enhances the activity of the catalyst and decreasing the activation energy [34] so we study the effect of K substitution over $LaZnO_y$. No work has been reported in the literature on the mixed La_2O_3 and ZnO catalyst for the oxidation of soot. Therefore, present paper is devoted for the first time to the study of kinetics of diesel soot oxidation over the mixed metal oxides having composition as $La_{0.7}K_{0.3}ZnO_y$ catalyst.

2. Material and Methods

2.1. Catalyst Preparation

A series of potassium promoted mixed metal oxides $La_{1-x}K_xZnO_y$ (x=0, 0.1, 0.2, 0.3 and 0.4) with similar stoichiometric composition as required for Perovskite formation $A_{1-x}K_xBO_3$ were prepared by the citric acid sol-gel method. All AR-grade chemicals were used in the preparation of catalysts. Aqueous solution (0.1 M) of $La(NO_3)_3.6H_2O$, $Zn(NO_3)_2.6H_2O$ and KNO_3 were mixed with citric acid that was equivalent in gram mole with that of the total cations (La^{3+}, Zn^{2+} and K^+). Resulting colorless solution was heated at 80 °C under continuous stirring. After 2-3 h of continuous stirring the clear solution gradually transformed into a gel which was translucent and viscous. The wet gel was dried homogeneously overnight in an air oven at 120 °C. Obtained off-white colored loose and foamy solid was heated at 450 °C for 4 h and further ground before calcining it at 750 °C for 4 h. Obtained solid was white colored porous material.

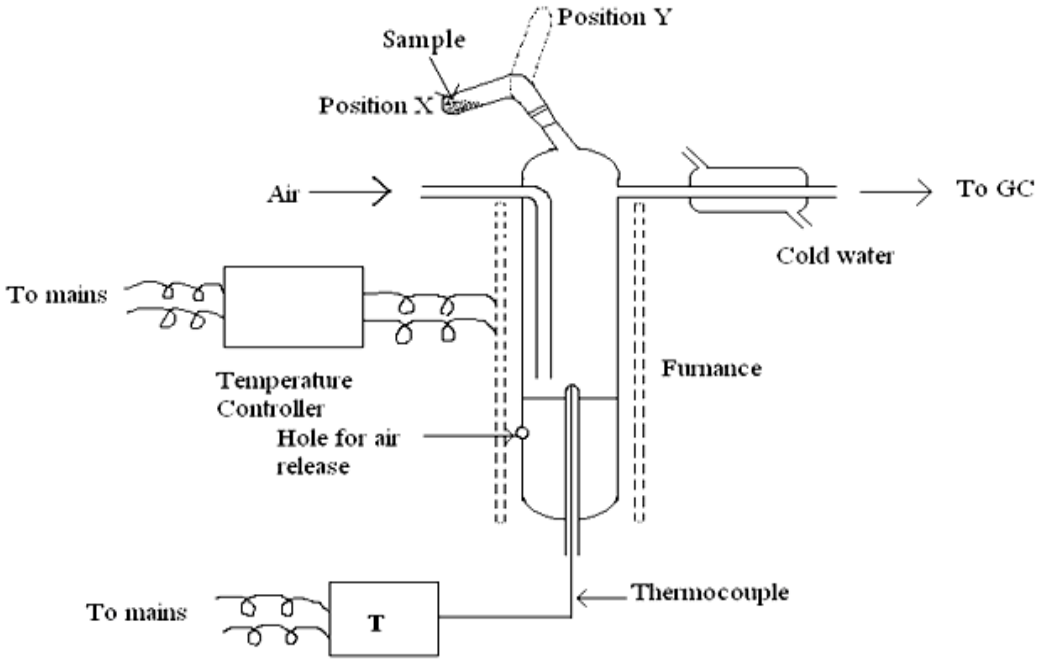

Figure 1. Schematic diagram of the semi-batch reactor

2.2. Soot Preparation

The real soot was prepared by partial combustion of commercial diesel (HP) in a lamp with limited supply of air which was deposited on the inner walls of an inverted beaker. The soot was collected from the recipient walls and then dried in an oven for overnight at 120 °C.

2.3. Bench Scale Reactor

Experimental set-up for collecting kinetic data under isothermal air oxidation of soot is shown in Figure 1. It was consisted of a tubular furnace with a microprocessor based temperature controller, a specially designed quartz reactor and a condenser for condensing water vapour and cooling the product gas to room temperature. The reactor has a sample tube (Fig. 1) attached to it by B-14 socket joint and a thermocouple well for measuring the temperature of the soot-catalyst bed. The bends of the sample tube and the tube connecting the sample tube to the reactor are such that when the sample tube is at position Y, the solid sample falls into the reactor. The outlet of the reactor is connected to a cooler cum condenser as shown in the figure. The furnace temperature can be controlled to ±0.5 °C and the temperature of the bed is measured by a thermocouple connected to a separate temperature indicator (T). There is a hole in the lower part of the outer tube of the reactor, to take care of breakage due to the expansion or contraction of air in between co-axial tubes as the unit is subjected to the variation of temperature from ambient to the reaction temperature.

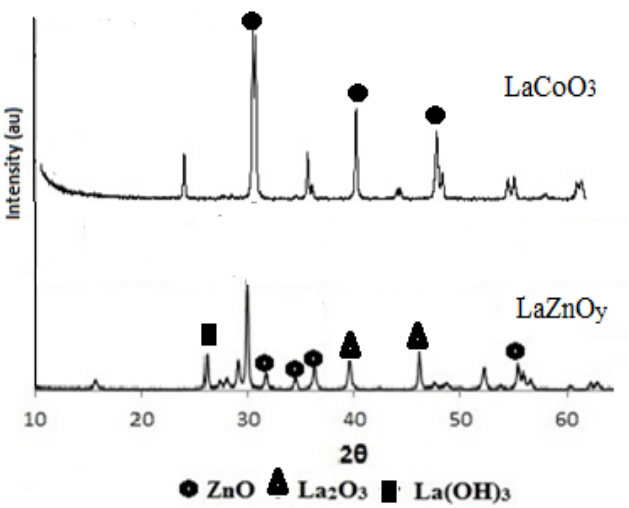

Figure 2. XRD patterns of mixed oxides of La/Zn and perovskite ($LaCoO_3$)

2.4. Experimental Procedure

A known weight of the soot-catalyst mixture was taken in the sample tube and it was connected to the system (position X). Before the oxidation reaction, the soot-catalyst mixture, in a 1/10 weight ratio, were milled in an agate

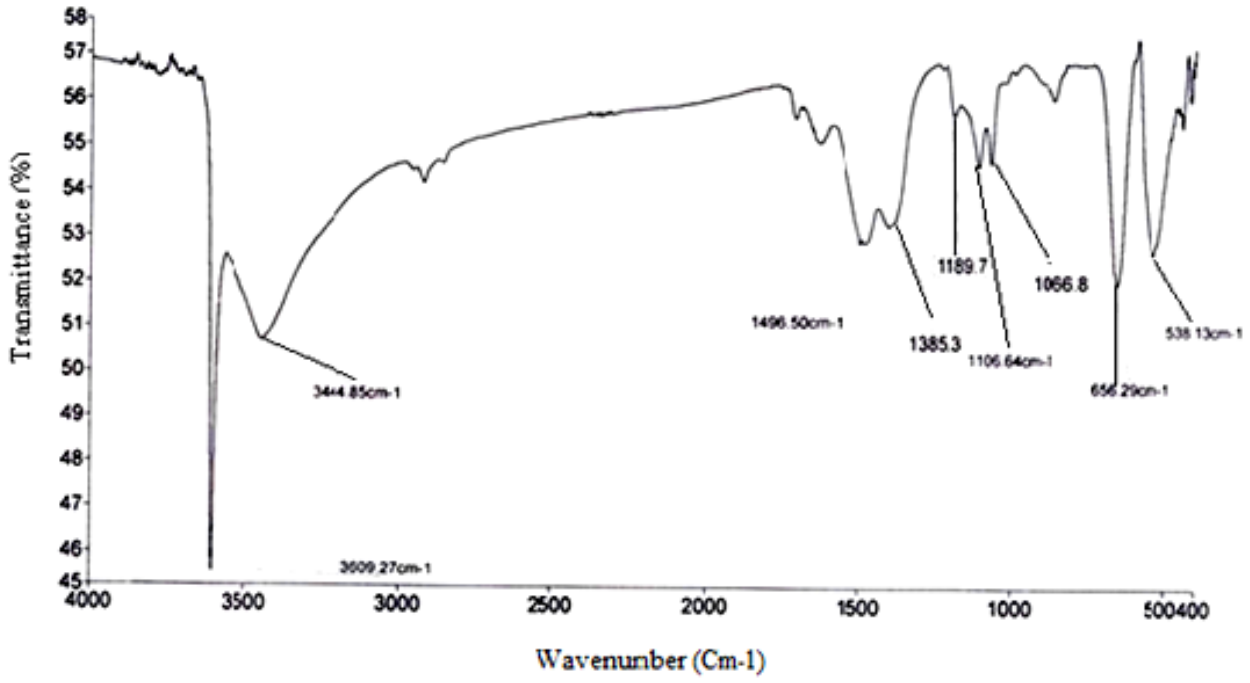

Figure 3. FTIR analysis of $La_{0.7}K_{0.3}ZnOy$

mortar for "tight contact". 110 mg of this catalyst-soot mixture was placed in the sample tube. The heating of the furnace was started and the dry and the CO_2 free air was fed at a flow rate of 150 ml/min. When the reactor attained the required temperature shown by the temperature indicator (T) the sample was dropped in the reactor by turning the sample tube by 180 ^{o} (i.e. position Y) and the Gaseous products were analyzed by a gas chromatograph as a function of time. The isothermal catalytic soot oxidation data were collected in the temperature range of 320-350 ^{o}C.

2.5 Catalyst Characterization

Prepared catalyst samples are characterized by FTIR, SEM and XRD to identify the structure and functional group of the sample prepared.

3. Results and Discussion

3.1. Characterization of Catalyst by XRD

It is interesting to note that the equimolar ratio of La and Zn was taken with the aim to prepare perovskite structure of $LaZnO_3$, instead of expectation perovskite phase is totally inaccessible. It is also very clear from the comparative studies of XRD of $LaZnO_Y$ with perovskite of $LaCoO_3$ catalyst prepared by sol gel method (Figure 2) that oxides of La and Zn did not form perovskite structure. Figure 2 shows that $LaCoO_3$ catalyst exhibited the typical XRD peaks of the rhombohedral perovskite structure (JCPDS No 84-0848).

3.2. Characterization of Catalyst by FTIR

The FTIR spectroscopy was employed as an additional probe to evidence the presence of OH groups as well as other organic and inorganic species present in the metal oxides. The FTIR spectrum in the range 4000-400 cm^{-1} of the catalyst, $La_{0.7}K_{0.3}ZnO_y$ is shown in Figure 3. An intense and sharp band at 3609.4 cm^{-1} is assigned to the stretching and bending O–H vibrations of lanthanum hydroxide [22-25]. Bands near 3444 cm^{-1} represent the O–H stretching mode indicative of the presence of adsorbed water on the sample surface [26] and peaks at 1496 and 1385 cm^{-1} show $La_2O_2CO_3$ [27]. The strong peak at 1066 cm^{-1} is assigned to the Zn–O–H bending. The characteristics

Table 2. Light off Temperatures of $La_{1-x}K_xZnO_y$ Catalyst

Catalysts	T_i (^{o}C)	T_{50} (^{o}C)	T_{100} (^{o}C)
$LaZnO_y$	376	426	456
$La_{0.9}K_{0.1}ZnO_y$	317	369	400
$La_{0.8}K_{0.2}ZnO_y$	258	300	333
$La_{0.7}K_{0.3}ZnO_y$	204	280	329
$La_{0.6}K_{0.4}ZnO_y$	236	290	322

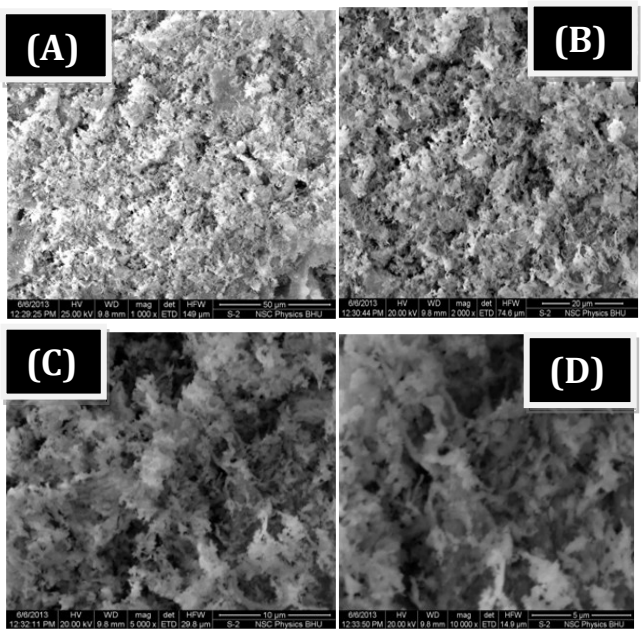

Figure 4. SEM images of $La_{0.7}K_{0.3}ZnO_Y$ catalyst: (A) 1000x; (B) 2,000x; (C) 5,000x; (D) 10,000x magnification

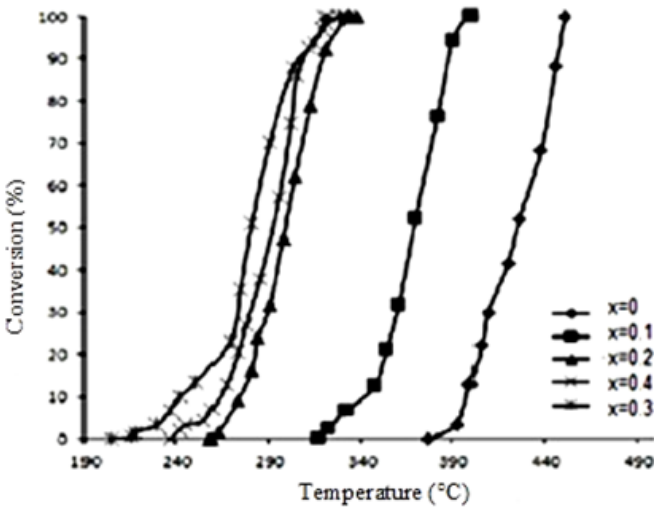

Figure 5. Soot conversion over $La_{1-x}K_xZnO_y$ (x = 0-0.4), calcination 750 ^{o}C, catalyst/soot: 10/1, tight contact, air flow rate: 150 ml/min

peaks at 538.13 cm^{-1} and 656.29 cm^{-1} show presence of ZnO and La_2O_3 [28, 29]. Thus ZnO and La_2O_3 remained as mixture; they did not form perovskite structure.

3.3. Characterization of $La_{0.7}K_{0.3}ZnO_y$ Catalyst by SEM

The SEM micrographs, at different magnifications, of K doped La_2O_3 and ZnO composite catalyst is displayed in Figure 4 ((A), (B), (C) and (D)). The SEM images show that the prepared catalyst sample was highly porous and less aggregated. The figure shows that the surface of the catalyst appears to be spongy tendrils. It can also be seen in lower magnification images (Figure 4A) that the particle size of the mixed oxides is small and uniformly distributed. The average particle size of the catalyst is about 100-120 nm, close to that for diesel soot particulates (70-100 nm), which is favorable to achieving the highest specific number of contact points between the two counterparts.

3.4. Catalytic Combustion of Soot over $La_{1-x}K_xZnO_y$ Catalysts

Experiments were conducted on a series of potassium promoted mixed metal oxides $La_{1-x}K_xZnO_y$ (x = 0-0.4) for soot oxidation and effect on the activity of catalyst with increasing amount of K was studied. Figure 5 shows the percent conversion of soot on various $La_{1-x}K_xZnOy$ catalysts. The effect of addition of K in the catalyst on the light off temperatures is recorded in Table 2. Activity of catalyst increased with increasing K from x = 0-0.3 and with further increase for x = 0.4 the activity decreased as shown in Figure 5 and it is also evident from Table 2. Therefore the optimum value of K in the catalyst is for x = 0.3.

Table 3. Characteristics temperatures for soot oxidation of pure oxides

Catalysts	T_i (°C)	T_{50} (°C)	T_{100} (°C)
La_2O_3	389	435	461
ZnO	406	441	474
$LaZnO_y$	376	426	456

3.5. Comparative Soot Oxidation on La_2O_3, ZnO and $LaZnO_y$

In order to investigate the effect of individual constituents of the $LaZnO_y$ in the oxidation reaction of soot, La_2O_3 and ZnO were also tested under same experimental condition. Figure 6 shows the percent conversion of soot over three catalysts viz $LaZnO_y$, La_2O_3 and ZnO. The nature of conversion curve of $LaZnO_y$ is similar to that of La_2O_3 and ZnO, not intersecting each other. It is very clear from the conversion of soot over composite oxide ($LaZnO_y$) is higher than its individual component at all the temperatures. The light off characteristics is summarized in Table 3. From table it can be seen that $LaZnO_y$ started soot oxidation (T_i) at 376 °C earlier by an amount of 13 °C and 30 °C with respect to ZnO and La_2O_3 respectively. Also $LaZnO_y$ perform better than their constituent oxides by giving complete oxidation at, T_{100} = 456 °C while T_{100} for La_2O_3 and ZnO are 461 and 474 °C respectively. The synergistic effect detected can be attributed to the morphology of the catalyst, spongy tendrils found in the SEM images (figures) helps to capture the soot

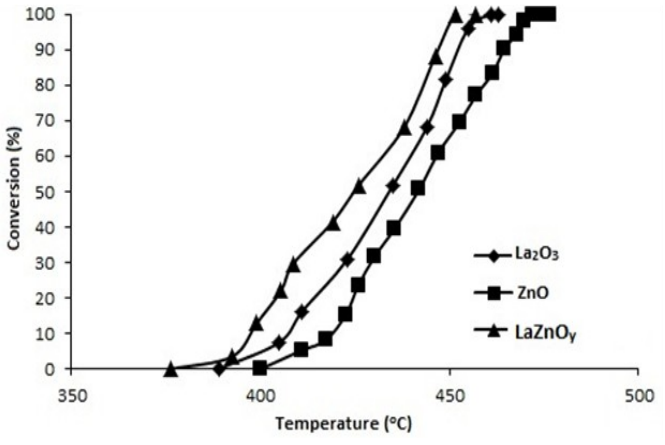

Figure 6. Synergistic effect of $LaZnO_y$ on soot oxidation. Calcination temperature 750 °C, catalyst/soot: 10/1, tight contact, air flow rate: 150 ml/min

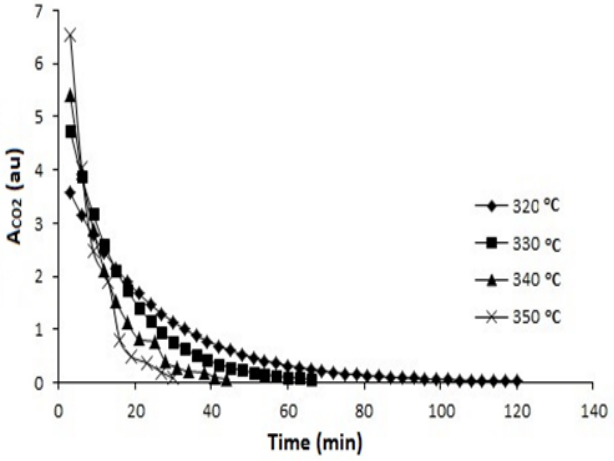

Figure 7. Plot of chromatogram area of CO_2 (A_{CO2}) vs time at four constant temperatures over $La_{0.7}K_{0.3}ZnO_y$

particle and gives more intimate contact of catalyst and soot.

3.6. Kinetics Study

The kinetics of catalyzed soot oxidation with air was studied under isothermal conditions as described above. Temperature range chosen for performing kinetic study is predicted from below mentioned light off temperatures of $La_{0.7}K_{0.3}ZnO_y$ catalyst (Table 2). The screening of the prepared catalysts showed that $La_{0.7}K_{0.3}ZnO_y$ was the most active for soot oxidation under the experimental conditions studied. Therefore, $La_{0.7}K_{0.3}ZnO_y$ catalyst in tight contact with soot was chosen to determine the kinetic model, activation energy and Arrhenius constant of the oxidation reaction as discussed below.

3.6.1. Determination of kinetic model

Figure 7 shows the chromatogram area at varying time obtained during experiment at four different constant temperatures (320, 330, 340 and 350 °C). Here as temperature increases the time required for complete oxidation of soot decreases due to higher rate of oxidation at higher temperature.

The fractional conversion of soot, (α) is defined as:

$$\alpha = (m_o\text{-}m)/m_o \quad (1)$$

where, m and m_o are the running and the initial sample mass respectively. The value of α at various extent of reaction is calculated using the following formula:

$$\alpha = \sum_0^t A_{CO2}\,\Delta t / \sum_0^{\infty} A_{CO2}\,\Delta t \quad (2)$$

where, Δt is the time differences. The empirical rate law equations as favored by Levenspiel [30] have been used to derive the kinetic parameters of diesel soot oxidation. The most general rate equation of solid-state reaction as given by Equation (3).

$$d\alpha/dt = k\,f(\alpha) \quad (3)$$

where α is fractional conversion, k is the reaction rate constant at any temperature and $f(\alpha)$ is any function of conversion. The assumption often made in the literature [31] is that the global soot oxidation rate in large excess oxygen can be described by a first order kinetic equation with respect to fraction conversion of soot, (α). In the present study flowing oxygen was in large excess, therefore Equation (3) becomes pseudo first order:

$$d\alpha/dt = k\,\alpha \quad (4)$$

Integrating Equation (4) we get:

$$\ln \alpha = kt \quad (5)$$

Calculating α from Equation (2) and plotting Equation (5) as ln α vs. t, one should get a straight line passing through the origin. Figure 8 shows such plot for the first order kinetics of soot oxidation.

These results obtained are best fit models having a high regression coefficient. Slope of the straight lines gives the values of reaction rate constants, 'k' at different temperatures.

3.6.2. Determination of activation energy

The kinetic rate constant 'k' in the model Equation (4) is temperature dependent and expressed by Arrhenius equation (Equation 6):

$$k = A e^{-(E/RT)} \quad (6)$$

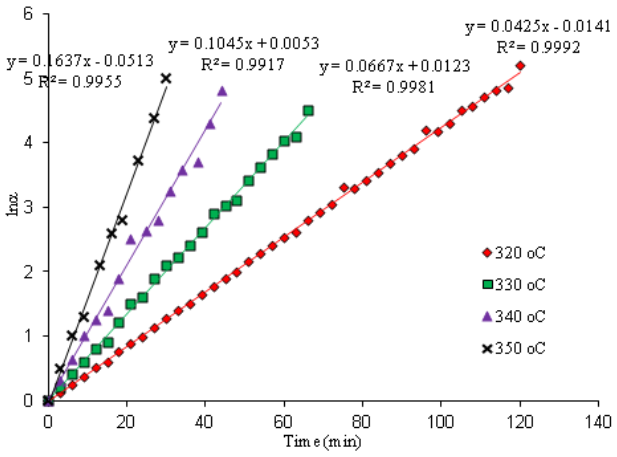

Figure 8. First order kinetics model for catalytic oxidation of soot at different temperature

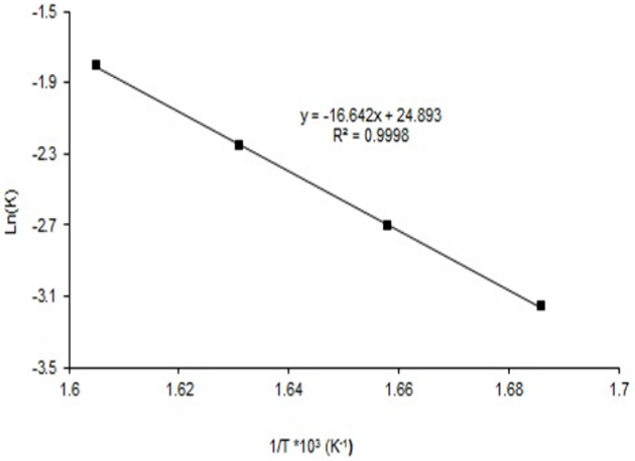

Figure 9. Arrhenius plot for catalytic oxidation of soot

where A is the frequency factor, E is activation energy, T is absolute temperature, R is the gas constant. On taking log of Equation (6), it can be written as Equation (7):

$$ln\, k = ln\, A - \frac{E}{RT} \quad (7)$$

and at two different temperatures this equation modifies to Equation (8):

$$\frac{k1}{k2} = e^{-\frac{E}{R}\left(\frac{1}{T_1}-\frac{1}{T_2}\right)} \quad where\ T_2>T_1 \quad (8)$$

The obtained value of k when fitted in Equation (7) gives straight line also known as Arrhenius plot as shown in the Figure 9. The slope of the straight line 'S' is related to activation energy which can be given as follows (Equation (9)):

$$S = -\frac{E}{R} \quad (9)$$

With the help of Arrhenius plot obtained value of activation energy, E = 138 kJ/mol. The value of the activation energy obtained is lower than that reported by various previous authors. Again using Equation (7) for two different temperatures frequency factor 'A' was calculated which is equal to 6.46×10^{10}. Thus the rate of catalytic oxidation of soot can be written as follows:

Rate = 6.46×10^{10} exp (-138 kJ/RT)(α) g.soot/ (g cat. min).

4. Conclusions

Soot oxidation was studied in a specially designed mini semi-batch reactor. The study of soot oxidation kinetics in the mini-scale reactor revealed that it assures practically isothermal conditions. Kinetics data were collected under the conditions of free heat and mass transfer limitations. Intrinsic reaction rate of air oxidation of diesel soot over $La_{0.7}K_{0.3}ZnO_y$ catalyst was determined as a function of temperature and fractional conversion in the temperature range of 320-350 ^oC, given by:

Rate = 6.46×10^{10} exp (-138 kJ/RT)(α) g.soot/ (g cat. min).

The value of activation energy was found to be 138 kJ/mol which was found the least compared with the reported activation energy for different catalysts in the literature.

Acknowledgment

The authors gratefully acknowledge the financial support given to the project by the Department of Science and Technology, India under the SERC (Engineering Science) project grant DST No: SR/S3/CE/0062/2010.

References

[1] Mishra, A., Prasad, R. (2014). Preparation and Application of Perovskite Catalysts for Diesel Soot Emissions Control: An Overview. *Catalysis Reviews: Science and Engineering*, 56(1): 57-81.

[2] Stamatelos, A.M. (1997). A review of the effect of particulate traps on the efficiency of vehicle diesel engines. *Energy Conversion Management*, 38: 83-99.

[3] Fino, D. (2007). Diesel emission control: A review of catalytic filters for particulate removal. *Science and Technology of Advance Materials*, 8: 93-100.

[4] Lopez-Fonseca, R., Elizundia, U., Lnda, I., Gutierrez-Ortiz, M.A., Gonzalez-Velasco, J.R. (2005). Kinetic analysis of non-catalytic and Mn-catalysed combustion of diesel soot surrogates. *Applied Catalysis: B*, 61: 50-158.

[5] Van Setten, B.A.A.L., Schouten, J.M., Makkee, M, Moulijn, J.A. (2000). Realistic contact for soot with an oxidation catalyst for laboratory studies. *Applied Catalysis: B*, 28: 253-257.

[6] Darcy, P., Da Costa, P., Mellotte, H., Trichard, J.M., Djega-Mariadassou, G. (2007). Kinetics of catalyzed and non-catalyzed oxidation of soot from a diesel engine. *Catalysis Today*, 119: 252-256.

[7] Stanmore, B.R., Brilhac, J.F., Gilot, P. (2001). the oxidation of soot: a review of experiments, mechanisms and models. *Carbon*, 39: 2247-2268.

[8] Dernaika, B., Uner, D. (2003). A simplified approach to determine the activation energies of uncatalyzed and catalyzed combustion of soot. *Applied Catalysis: B*, 40: 219-229.

[9] Illekova, E., Csomorova, K. (2005). Kinetics of oxidation in various forms of carbon. *Journal of Thermal Analysis and Calorimetry*, 80: 103-108.

[10] Lopez-Fonseca, R., Landa, I., Gutierrez-Ortiz, M.A., Gonzalez-Velasco, J.R. (2005). Non- isothermal analysis of the kinetics of the combustion of carbonaceous materials. *Journal of Thermal Analysis and Calorimetry*, 80: 65-69.

[11] Messerer, A., Niessner, R., Poschl, U. (2006). Comprehensive kinetic characte- rization of the oxidation and gasification of model and

real diesel soot by nitrogen oxides and oxygen under engine exhaust conditions: Measurement, Langmuir-Hinshelwood, and Arrhenius parameters. *Carbon*, 44: 307-324.

[12] Ahlstrom, A.F., Odenbrand, C.U.I. (1989). Combustion characteristics of soot deposits from diesel engines. *Carbon*, 27: 475-483.

[13] Du, Z., Sarofim, A.F., Longwell, J.P., Tognotti, L. (1991). in (ed). Lahaye, J., Ehrburger, P. in Control of Carbon Gasification Reactivity, In Fundamental Issues, Kluwer, Dordrecht.

[14] Du, Z., Sarofim, A.F., Longwell, J.P., Mims, C.A. (1991). Kinetic measurement and modeling of carbon oxidation. *Energy and Fuels*, 5: 214-221.

[15] Kalogirou, M., Samaras, Z. (2010). Soot oxidation kinetics from TG experiments. *Journal of Thermal Analysis and Calorimetry* 99: 1005-1010.

[16] Castoldi, L., Matarrese, R., Lietti, L., Forzatti, P. (2006). Simultaneous removal of NO_x and soot on Pt-Ba/Al_2O_3 NSR catalysts. *Applied Catalysis: B*, 64: 25-34.

[17] Russo, N., Furfori, S., Fino, D., Saracco, G., Specchia, V. (2008). Lanthanum cobaltite catalysts for diesel soot combustion. *Applied Catalysis B: Environmental*, 83: 85-95.

[18] Wang, H., Zha, Z., Liang, P., Xu, C., Duan, A., Jiang, G., Xu, J., Liu, J. (2008). Highly Active $La_{1-x}K_xCoO_3$ Perovskite-type Complex Oxide Catalysts for the Simultaneous Removal of Diesel Soot and Nitrogen Oxides under Loose Contact Conditions. *Catalysis Letters*, 124: 91-99.

[19] Li, Z., Meng, M., Li, Q., Xie, Y., Hu, T., Zhang, J. (2010). Fe-substituted nanometric $La_{0.9}K_{0.1}Co_{1-x}Fe_xO_3$ perovskite catalysts used for soot combustion, NO_x storage and simultaneous catalytic removal of soot and NO_x. *Chemical Engineering Journal* 164: 98-105.

[20] Sánchez Escribano, V., Fernández López, E., Gallardo-Amores, J.M., del Hoyo Martínez, C., Pistarino, C., Panizza, M., Resini, C., Busca, G.A. (2008). Study of a ceria-zirconia-supported manganese oxide catalyst for combustion of Diesel soot particles. *Combustion and Flame*, 153: 97-104.

[21] Dhakad, M., Mitshuhashi, T., Rayalu, S., Doggali, P., Bakardjiva, S., Subrt, J., Fino, D., Haneda, H., Labhsetwar, N. (2008). Co_3O_4-CeO_2 mixed oxide-based catalytic materials for diesel soot oxidation. *Catalysis Today*, 132: 188-193.

[22] Zhang, H.B., Liu. H.S., Cao, X.J., Li, S.J., Sun, C.C. (2003). Preparation and properties of the aluminum-substituted α-$Ni(OH)_2$. *Materials Chemistry and Physics*, 79: 37-42.

[23] Zhu, H.L., Yang, D.R., Yang, H., Zhu, L.M., Li, D.S., Jin, D.L., Yao, K.H. (2008). Reductive hydrothermal synthesis of $La(OH)_3$:Tb^{3+} nanorods as a new green emitting phosphor. *Journal of Nanoparticle Research*, 10: 307-312.

[24] Levan, T., Che, M., Tatibouet, J.M., Kermarec, M. (1993). Infrared Study of the Formation and Stability of $La_2O_2CO_3$ during the Oxidative Coupling of Methane on La_2O_3. *Journal of Catalysis*, 142: 18-26.

[25] Busca, G., Lorenzelli, V. (1982). Infrared spectroscopic identification of species arising from reactive adsorption of carbon oxides on metal oxide surfaces. *Journal of Materials Chemistry*, 7: 89-126.

[26] Zou, G., Liu, R., Chen, W., Xu, Z. (2007). Preparation and characterization of lamellar-like $Mg(OH)_2$ nanostructures via natural oxidation of Mg metal in formamide/water mixture. *Materials Research Bulletin*, 42: 1153-1158.

[27] Mu, Q., Wang, Y. (2011). Synthesis, characterization, shape-preserved transformation, and optical properties of $La(OH)_3$, $La_2O_2CO_3$, and La_2O_3 nanorods. *Journal of Alloys and Compounds* 509: 396-401.

[28] Fischer, C.H., Muffler, H.J., Bar, M., Fiechter, S., Leupolt, B., Lux-Steiner, M.C. (2002). Ion layer gas reaction (ILGAR) conversion, thermodynamic considerations and related FTIR analyses. *Journal of Crystal Growth*, 241: 151-158.

[29] Vasudevan, S., Lakshmi, J., Sozhan, G. (2013). Electrochemically assisted coagulation for the removal of boron from water using zinc anode. *Desalination*, 310: 122-129.

[30] Levenspiel, O. (1999). *Chemical Reaction Engineering*, III Edn, John Wiley & Sons. New York, 379-381.

[31] Neeft, J.P.A., Nijhuis, T.X., Smakman, E., Makkee, M., Moulijn, J.A. (1997). Kinetics of the oxidation of diesel soot. *Fuel*, 76(12): 1129-1136.

[32] Darcy, P., Da Costa, P., Mellotte, H., Trichard, J.M., Djega-Mariadassou, G. (2007). Kinetics of catalyzed and non-catalyzed oxidation of soot from a diesel engine. *Catalysis Today*, 119: 252-256.

[33] Lopez-Fonseca, R., Elizundia, U., Landa, I., Gutierrez-Ortiz, M.A., Gonzalez-Velasco, J.R. (2005). Kinetic analysis of non-catalytic and Mn-catalysed combustion of diesel soot surrogates. *Applied Catalysis B: Environmental*, 61: 150-158.

[34] Hernandez S, Andrea Blengini G, Russo N, Fino D (2012) Kinetic Study of Diesel Soot Combustion with Perovskite Catalysts. *Industrial and Engineering Chemistry Research*, 51: 7584-7589.